

SparseDR: Differentiable Rendering of Sparse Signed Distance Fields

First Author¹, Second Author², Third Author^{2,3} and Fourth Author⁴

¹First Affiliation

²Second Affiliation

³Third Affiliation

⁴Fourth Affiliation

{first, second}@example.com, third@other.example.com, fourth@example.com

Abstract

We present SparseDR, a differentiable rendering implementation designed for sparse representations based on Signed Distance Fields (SDF). We leverage the Sparse Brick Set (SBS) representation and propose an adaptation of redistancing and regularization of the SDF defined on SBS. This enables our method to surpass existing differentiable rendering implementations in accuracy at limited memory budgets by increasing the effective resolution of the SDF representation.

1 Introduction

Signed distance functions (SDFs) provide a continuous, implicit representation of geometry, defining the shortest Euclidean distance from any point in space to the nearest surface, with the sign indicating interior or exterior regions. This enables gradient-based optimization by supporting differentiable rendering, where ray marching samples distances to compute density and color, facilitating inverse rendering tasks such as shape and material recovery from images.

SDF-based differentiable rendering produces high-fidelity reconstructions with smooth surfaces and topological consistency, outperforming many existing methods in handling complex topologies. Unfortunately, existing SDF-based differentiable rendering implementations are constrained in reconstruction accuracy due to high memory consumption and substantial computational demands. Our work proposes a solution to this problem, alleviating limitations through better data structures and sampling techniques:

- We propose an adaptation of SDF-based differentiable rendering to a sparse data structure, which increases the effective resolution of the SDF representation and thereby improves the surface reconstruction accuracy.
- We provide two novel algorithms of redistancing: a full version for SBS in general and its accelerated version specifically for the differentiable rendering of SBS.

2 Related Work

[Vicini *et al.*, 2022] introduces differentiable rendering operating directly on an SDF representation. The authors modi-

fied sphere tracing so that, in addition to computing the surface intersection, it evaluates a special reparameterization of rays, enabling correct gradients with respect to shape parameters, including the visibility contribution of individual surface regions. This work also first proposed the use of a *redistancing* — a process of recomputing values on a grid such that all grid cells store correct distances to the surface. In differentiable rendering this recomputation is required because, after an optimization step and updating the distances at grid nodes, the grid no longer strictly represents an SDF. [Wang *et al.*, 2024] exploits properties of distance functions and estimate the boundary integral by an integral over a relaxed boundary, i.e., a thin band around the object silhouette. [Zhang *et al.*, 2025] propose for computing gradients in the presence of multiple surfaces along a ray path: instead of locally differentiating a single surface, the authors consider a volumetric, non-local perturbation of the surface.

All of the above methods represent the distance function volumetrically on a regular grid, which leads to three fundamental issues: (1) significant memory consumption, especially when using automatic differentiation frameworks such as DrJit [Jakob *et al.*, 2022] or PyTorch [Jason and Yang, 2024]; (2) slow ray–surface intersection based on sphere tracing; (3) an expensive redistancing algorithm that propagates modified SDF values across the entire grid.

Hash-table-based methods such as InstantNGP [Müller *et al.*, 2022] could mitigate the first issue, but by themselves cannot address the second and third. The key difficulty is that the data structure used to store the SDF directly constrains how differentiable ray–surface intersections are computed and how redistancing is performed, and implementing redistancing on hash tables is, in our view, highly nontrivial. Our work shows how these three components – data structure, ray intersection, and redistancing – can be joined together in an efficient manner.

3 Implementation Details

To store the surface, SparseDR uses the Sparse Brick Set (SBS) proposed in [Söderlund *et al.*, 2022], which is a hybrid of hierarchical and regular representations, see Figure 1. The entire scene is encoded as a BVH or an octree, while its leaves store small regular grids, for example 4x4x4 voxels (5x5x5 distances). For gradient computation, we adapt the relaxed boundary method from [Wang *et al.*, 2024], which we

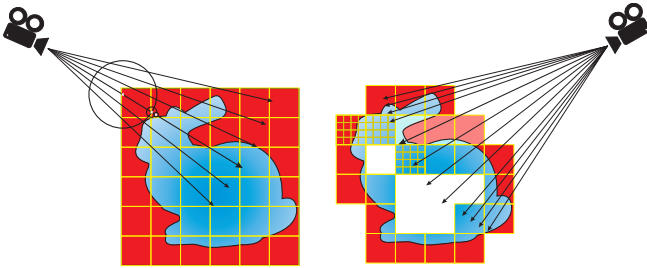


Figure 1: Comparison of SparseDR algorithm with the baseline. The baseline (on the left) uses dense SDF grid to represent the surface, and sphere tracing for ray-scene intersection. SparseDR (on the right) uses Sparse Brick Set, each brick stores small SDF grid, and a ray intersects each brick on its way until it hits the surface.

refer to as our baseline. At the beginning of the optimization process, the distance function is initialized with a sphere defined on a low-resolution grid (32x32x32). At each iteration, we estimate the gradient and update the distance values using a gradient descent step, followed by a regularization and accelerated redistancing (see Figure 2). On every iteration when upsampling is required, which is defined by the user, three steps are executed: sparsification step, full redistancing and upsampling. Sparsification and full redistancing are also applied before the resulting model is saved.

Gradient evaluation. The key distinction of the method underlying SparseDR lies in the transition from an SDF grid to a sparse brick set. In our case, each brick has a fixed size of $4 \times 4 \times 4$ voxels. For the SBS, a BVH tree is constructed, with each leaf node storing a single brick. In addition to sphere tracing, the Newton method [Söderlund *et al.*, 2022] for ray-SDF intersection has been implemented. It is specifically designed to find intersections inside the voxel. A ray first traverses the BVH; if an intersection with a leaf node is found, it then intersects the voxels of the brick. The ray traverses each brick along its path until it hits the surface or there are no bricks left.

The Newton method was modified to search for relaxed boundary points. According to [Wang *et al.*, 2024], a point belongs to the relaxed boundary if the SDF value at that point is below a certain threshold, which we refer to as the relaxed epsilon, and the SDF derivative along the ray reaches its local minimum. The Newton method is based on the fact that inside a voxel, the SDF along the ray can be represented as a cubic polynomial. Thus, within the voxel, a potential relaxed boundary point is found as the root of a quadratic equation, after which the SDF value at the point is checked to be less than the relaxed epsilon. The case when the local minimum occurs on the boundary between voxels or bricks is handled separately.

SparseDR is implemented in C++ and Vulkan and does not use automatic differentiation. The chain of computations that was differentiated is as follows: MSE loss – pixel color (an average of sample colors) – sample color (when it hits the surface: trilinear interpolation of distances in the voxel) – distances. Gradients are accumulated in a float array whose size equals the number of updated distances. In the shader, when computing the color of a pixel for 16 samples, information

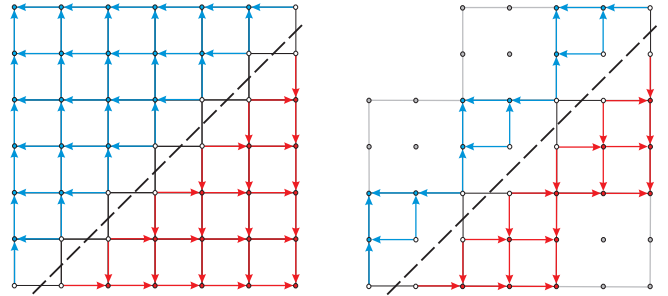


Figure 2: Comparison of the redistancing algorithm on grid (on the left) with the accelerated version (on the right) with SBS bricks 3×3 in size. The dots represent the distance values. Red and blue dots are the distances outside and inside the object respectively. Strip line represents the surface, set by distances colored white. Arrows show the order of updating the values. Bricks without surface (grey) are ignored by accelerated redistancing.

about the voxels hit by the samples is stored; after every 16 samples (or after the last one), the gradients are added to the array. SparseDR optionally uses an additional shader that samples only pixels containing boundaries and evaluates only the boundary integral, without the need for color computation. This adaptive boundary sampling allows cheaper samples and yields more accurate gradients for smaller relaxed epsilon values, thereby reducing bias.

Redistancing. For differentiable rendering of SBS in SparseDR, two versions of redistancing have been implemented. The first, full version, is an adaptation of the parallel fast sweeping method [Detrixhe *et al.*, 2013] for SBS, which is used to acquire the correct SDF. It addresses the problem of distance updates across empty space between bricks by additionally using extrapolation between brick faces. For each face of a brick without a direct neighbor, the nearest neighbor bricks are found, and one of their faces is selected for extrapolation. These neighbors are determined once, and after each fast sweeping step, values are extrapolated considering the grid spacing. From the extrapolated and previous values, the one with the smallest absolute value is chosen. To propagate the updated distances, the fast sweeping method is always applied as the final step of this algorithm.

However, using SBS instead of a grid and Newton’s method for intersection enables certain optimizations to the redistancing algorithm for the needs of differentiable rendering. First, it ignores the bricks without surface, and second, the value updates are localized within the bricks and not propagated between them. This accelerated version neither degrades reconstruction quality nor affects convergence to the reference.

The first version outputs correct sparse SDF, so it is used in SparseDR before upsampling and saving the result of reconstruction. The second version is faster while giving the same result, so it is applied on each iteration.

Sparsification and Upsampling. The sparsification step is performed before upsampling. During this stage, all bricks containing the surface are preserved, as well as all bricks within a radius of 1 voxel from them, including diagonal neighbors. If any of the adjacent bricks are missing, they

165 are added at this stage. This is necessary in cases where the
 166 reconstructed object contains fine details, so that the bricks
 167 where these details' reconstruction should reside would otherwise
 168 be absent. Thus, this step not only contributes to reducing
 169 the model size, but also eliminates a potential limitation
 170 compared to the baseline method. After the sparsification
 171 step, the full version of redistancing is applied to recom-
 172 pute all distances before upsampling or saving the resulting
 173 SBS, ensuring that the model represents a valid SDF. The up-
 174 sampling step doubles the resolution of the remaining bricks,
 175 generating eight new bricks from each original one. The new
 176 distance values are computed using trilinear interpolation.

177 4 Experiments

178 Experiments with the baseline method were conducted us-
 179 ing the official implementation from [Wang, 2024]. The
 180 baseline method employed the hyperparameters specified in
 181 the paper [Wang *et al.*, 2024], while the remaining parame-
 182 ters were taken from the configuration file “turbo.json”. The
 183 only modifications concerned the number of viewpoints, the
 184 batch size, and the upsampling iterations. For consistency
 185 across experiments, an identical lighting setup was used:
 186 two directional light sources with directions $(1, 1, 1)$ and
 187 $(-1, -1, -1)$, along with ambient light. The experiments
 188 were carried out on six models. Reconstruction used 16 view-
 189 points uniformly distributed over a sphere around the scene,
 190 generated by the algorithm from [Wang, 2024]. The batch
 191 size is 4 viewpoints, image resolution is 1024×1024 . The full
 192 optimization process comprised 1000 steps, with upsampling
 193 applied at steps 200, 400, 600, 700, 800, and 900. Computa-
 194 tions were performed on an AMD Ryzen 9 7950X CPU and
 195 an NVIDIA GeForce RTX 4090 GPU.

196 5 Conclusion

197 In this work we present SparseDR, a system for 3D recon-
 198 struction based on the method of differentiable rendering for
 199 a sparse SDF representation. Using [reference] as a base-
 200 line, we leverage the advantages of SBS and modify all stages
 201 of the algorithm. As a result, SparseDR achieves perfor-
 202 mance and reconstruction quality comparable to the original
 203 approach while reducing memory consumption by an order of
 204 magnitude. Future work will focus on upgrading SparseDR
 205 to a full-fledged path tracer and addressing the challenges that
 206 complicate the practical use of differentiable rendering, in
 207 particular the need for precise camera parameter information.

208 References

- 209 [Detrixhe *et al.*, 2013] Miles Detrixhe, Frédéric Gibou, and
 210 Chohong Min. A parallel fast sweeping method for the
 211 eikonal equation. *Journal of Computational Physics*,
 212 237:46–55, 2013.
- 213 [Jakob *et al.*, 2022] Wenzel Jakob, Sébastien Speierer, Nico-
 214 las Roussel, and Delio Vicini. Dr.jit: a just-in-time com-
 215 piler for differentiable rendering. 41(4), 2022.
- 216 [Jason and Yang, 2024] Jason and Edward He et al. Yang.
 217 Pytorch 2: Faster machine learning through dynamic
 218 python bytecode transformation and graph compilation. In

*Proceedings of the 29th ACM International Conference
 on Architectural Support for Programming Languages
 and Operating Systems, Volume 2, ASPLOS ’24, page
 929–947, New York, NY, USA, 2024. Association for
 Computing Machinery.*

[Müller *et al.*, 2022] Thomas Müller, Alex Evans, Christoph
 Schied, and Alexander Keller. Instant neural graphics
 primitives with a multiresolution hash encoding. *ACM
 Trans. Graph.*, 41(4), 2022.

[Söderlund *et al.*, 2022] Herman Hansson Söderlund, Alex
 Evans, and Tomas Akenine-Möller. Ray tracing of signed
 distance function grids. *Journal of Computer Graphics
 Techniques Vol.*, 11(3), 2022.

[Vicini *et al.*, 2022] Delio Vicini, Sébastien Speierer, and
 Wenzel Jakob. Differentiable signed distance function ren-
 dering. *ACM Trans. Graph.*, 41(4), July 2022.

[Wang *et al.*, 2024] Zichen Wang, Xi Deng, Ziyi Zhang,
 Wenzel Jakob, and Steve Marschner. A simple approach to
 differentiable rendering of sdfs. In *SIGGRAPH Asia 2024
 Conference Papers*, New York, NY, USA, 2024. Associa-
 tion for Computing Machinery.

[Wang, 2024] Zichen Wang. A simple approach to differen-
 tiable rendering of sdfs repository, 2024.

[Zhang *et al.*, 2025] Ziyi Zhang, Nicolas Roussel, and Wenzel
 Jakob. Many-worlds inverse rendering. *ACM Trans.
 Graph.*, 45(1), October 2025.